Geochemistry Geophysics Geosystems G3

Article
Volume 12, Number 6
24 June 2011
Q06014, doi:10.1029/2011GC003533
ISSN: 1525-2027

Published by AGU and the Geochemical Society

Understanding sedimentation in the Song Hong–Yinggehai Basin, South China Sea

Yi Yan
Key Laboratory of Marginal Sea Geology, Guangzhou Institute of Geochemistry, Chinese Academy of Sciences, Guangzhou 510640, China (yanyi@gig.ac.cn)

Andrew Carter
Department of Earth and Planetary Sciences, Birkbeck College, University of London, Malet Street, London WC1E 7HX, UK

Carl Palk
Department of Earth Sciences and Engineering, Imperial College, Royal School of Mines, Prince Consort Road, London SW7 2BP, UK

Stéphanie Brichau
LMTG, Université Paul Sabatier, F-31000 Toulouse, France

Xiaoqiong Hu
Key Laboratory of Marginal Sea Geology, Guangzhou Institute of Geochemistry, Chinese Academy of Sciences, Guangzhou 510640, China

[1] The Cenozoic Song Hong–Yinggehai Basin in the South China Sea contains a large volume of sediment that has been used in previous studies, together with regional geomorphology, to argue for the existence of a large palaeodrainage system that connected eastern Tibet with the South China Sea. To test this and to understand the significance of sediment volumes deposited in the Song Hong–Yinggehai Basin, this study compared erosion histories of source regions with sediment volumes deposited during the two main stages in basin evolution spanning active rifting and subsidence (30–15.5 Ma) and postrift sedimentation (15.5 Ma to present). The study of basin provenance by detrital zircon U-Pb dating revealed Hainan was an important and continuous source of sediment, and a bedrock thermochronological study quantified its overall contribution to basin sedimentation. Comparison between the accumulated mass of basin sediment and volumes of eroded bedrock, calculated from apatite thermochronometry across the modern Red River drainage in northern Vietnam as well as Hainan Island, accounted for the bulk of sediment deposited since 30 Ma. Consequently, if an expanded paleodrainage ever existed it must have predated the Oligocene.

Components: 8700 words, 9 figures, 3 tables.

Keywords: Hainan; Red River; South China; low-temperature thermochronology; zircon U-Pb.

Index Terms: 1140 Geochronology: Thermochronology; 5475 Planetary Sciences: Solid Surface Planets: Tectonics (8149); 8175 Tectonophysics: Tectonics and landscape evolution.

Received 28 January 2011; **Revised** 5 May 2011; **Accepted** 5 May 2011; **Published** 24 June 2011.

Yan, Y., A. Carter, C. Palk, S. Brichau, and X. Hu (2011), Understanding sedimentation in the Song Hong–Yinggehai Basin, South China Sea, *Geochem. Geophys. Geosyst.*, *12*, Q06014, doi:10.1029/2011GC003533.

1. Introduction

[2] Sedimentary flux changes in offshore basins represent a large and complicated system sensitive to interplay between climate, tectonics and changes to regional drainage involving river capture or diversion. A prime example of these interactions can be found in the NW-SE aligned Song Hong–Yinggehai Basin located in the Gulf of Tonkin, northwestern South China Sea (Figure 1), which developed in response to strike-slip tectonics associated with the India-Asia collision through southeastward slip and clockwise rotation of the Indochina block along the Ailao Shan–Red River Fault zone (RRFZ) and related structures. The basin contains large thicknesses of sedimentary rocks, up to 16 km in the center (Figure 2), the bulk of which was deposited since 35 Ma [*Gong and Li*, 1997, 2004; *Hao et al.*, 1998; *Xie et al.*, 2001; *Clift and Sun*, 2006]. Studies of seismic reflection data show basin sedimentation rates increased between 29.5 and 21 Ma, fell between 21 and 15.5 Ma, and rose once more between 15.5 and 10.5 Ma with peak sedimentation rates in the Plio-Pleistocene [*Clift and Sun*, 2006; *Huang and Wang*, 2006; *van Hoang et al.*, 2010]. Most studies have sought to explain these changes as responses to changes in intensity of the East Asian Monsoon or local tectonics based on temporal associations.

[3] Monsoon intensification has been suggested for the Middle to Late Miocene rises in sediment flux, since this is a common feature across South, Southeast and East Asia [*Clift*, 2006] but before this local tectonics, related to continental extrusion of Southeast Asia may have been more important [*Clift and Sun*, 2006]. Climate proxy records for the East Asian Monsoon based on chemical weathering intensity from ODP cores in the tectonically stable Pearl River Mouth Basin (ODP site 1148) [*Li et al.*, 2003; *Wan et al.*, 2007] show arrival of a strong (wet) summer monsoon took place between 22 and 17 Ma [*Clift et al.*, 2008a; *van Hoang et al.*, 2010; *Wei et al.*, 2006]. This would be expected to produce a rise in sedimentation rates in the Song Hong–Yinggehai Basin but the opposite has been observed.

[4] There is also the possibility that sediment flux was affected by changes in the size of the paleo river system based on geomorphological studies along the margins of eastern Tibet which led to the proposal that the modern rivers draining the plateau margin were once tributaries to a single, southward flowing system that drained into the South China Sea [*Clark et al.*, 2004] via the paleo Red River, with the Song Hong–Yinggehai Basin as the main sediment depocenter. Disruption of the paleodrainage by river capture and reversal prior to or coeval with the initiation of surface uplift in eastern Tibet, possibly in the Miocene, then shrank this drainage and in the process less sediment was transported to the marine basins (Figure 3). However, timing of capture and scale of the original drainage are open to question. For example it has been argued on the basis of thermochronometric data that capture of the middle Yangtze by the lower Yangtze, beheading the Red River, took place in the Eocene [*Richardson et al.*, 2010]. Another study argued that drainage changes dated to the Oligocene, based on mass balance between estimated depths of erosion relative to a regional planation surface and deposited rock volumes in the South China Sea basins [*Clift et al.*, 2006].

[5] To unravel these different influences requires detailed understanding of both source and sink. The latter is reasonably well constrained and the most recent study calculated 385,000 km^3 of clastic material has been deposited in the Song Hong–Yinggehai Basin since 30 Ma [*van Hoang et al.*, 2010]. Adjusted for loss by chemical weathering [e.g., *Moon et al.*, 2007] this value is equivalent to 504,350 km^3 of eroded rock (Table 1) which if distributed across a drainage area similar to the present-day catchment of the Red River (~143,000 km^2) represents about 3.53 km of denudation since 30 Ma, or less if the paleodrainage was once larger. Whether this estimate is realistic is unknown as no direct evidence has yet been presented to constrain the paleo river drainage area and define the magnitude of contributions from source areas. It is not known if the drainage area of the paleo Red River or its equivalent was of similar size to the present or much larger. Furthermore, contributions from other source areas such as Hainan Island and the Vietnam margin to the west remain unknown quantities.

[6] To understand the significance of sediment volumes deposited in the Song Hong–Yinggehai Basin this study compared erosion histories of the potential source regions with sediment volumes deposited during the two main stages in basin evolution spanning active basin rifting and subsidence coupled with movement of the RRFZ (34–16 Ma) and postrift sedimentation (15.5 Ma to present) after extrusion had ended. To monitor sediment provenance we applied detrital zircon U-Pb dating to core samples from the Song Hong–Yinggehai

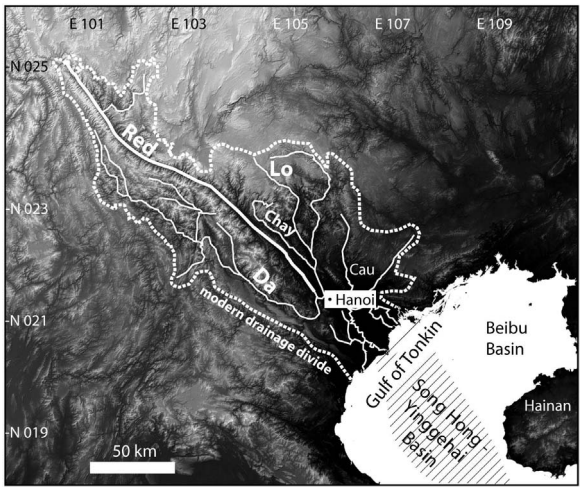

Figure 1. The Red River drainage and location of the Song Hong–Yinggehai Basin.

Basin and conducted a thermochronological study of bedrock exhumation across Hainan to define the contribution of this island to overall basin sedimentation.

2. Red River Fault Zone and Basin Evolution

[7] The Song Hong–Yinggehai Basin (Figure 2) is one of the largest pull-apart basins in the world that developed in response to strike-slip deformation as a result of the collision and indentation of India into Asia [*Molnar and Tapponnier*, 1975; *Tapponnier et al.*, 1986]. Indentation led to southeastward slip and clockwise rotation of the Indochina block along NW-SE striking faults, including the 1000 km long left-lateral Ailao Shan–Red River fault that runs from the southeastern corner of Tibet to the South China Sea. Deformation and extrusion took place in the Oligocene and Miocene [*Tapponnier et al.*, 1986, 1990, 2001; *Leloup et al.*, 1995, 2001; *Wang and Burchfiel*, 1997; *Gilley et al.*, 2003] but how the deformation was accommodated remains controversial [*Searle*, 2006; *Searle et al.*, 2010]. Views also differ as to how the Cenozoic deformation associated with strike-slip tectonics affected basin development. Some regarded basin evolution as tied to coupling between strike-slip tectonics and the rifting linked to opening of the South China Sea [*Guo et al.*, 2001; *Sun et al.*, 2003, 2004; *Replumaz and Tapponnier*, 2003], while others considered that most of the extension that drove basin formation was independent of the strike-slip tectonics and more closely associated with the opening of the South China Sea, especially during the Miocene, driven by subduction forces to the south [e.g., *Morley*, 2002; *Clift et al.*, 2008b]. However, there is general agreement on basin structure, stratigraphy and subsidence history.

[8] Sedimentation in the Song Hong–Yinggehai Basin is normally divided into synrift and postrift sequences since extensional tectonics appears the dominant control on basin formation. Seismic reflection lines show a basin-wide angular unconformity [*Zhu et al.*, 2009] which separates faulted Eocene to Early Miocene synrift sequences from relatively uniform postrift strata. Although basement subsidence began at or before 45 Ma the main period of subsidence, associated with transtensional faulting, began around 35 Ma [*Xie et al.*, 2001] coincident with initiation of movement on the Red River Fault Zone [*Gilley et al.*, 2003]. The main depocenters show a general migration to the southeast until interrupted by fault reversal at 16 Ma, which led to basin inversion, formation of an angular unconformity and migration of depocenters back to the northwest. Slowdown of dextral movement and high rates of sediment supply led to overspill to the east into the Qiongdongnan basin [*Clift and Sun*, 2006; *Xie et al.*, 2008], and soon after depocenter migration returned to a southward drift [*Zhu et al.*, 2009]. A prevailing southerly

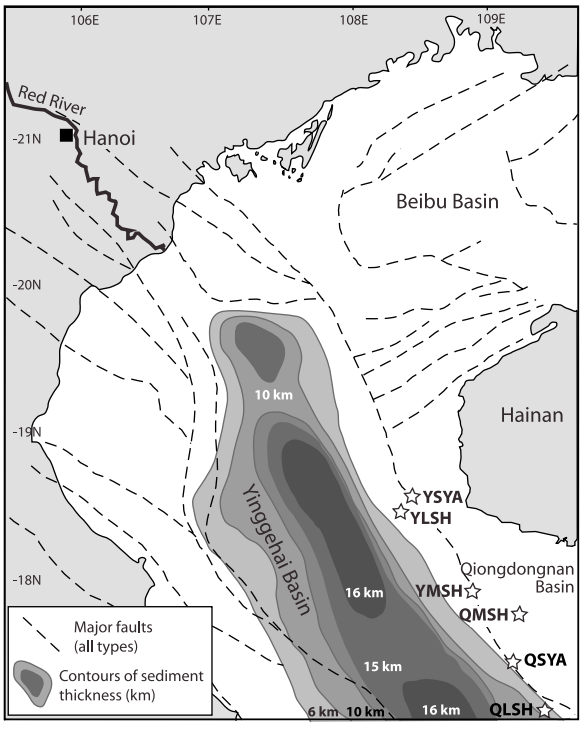

Figure 2. Location of studied well samples from the Song Hong–Yinggehai Basin in the South China Sea. Sediment isopachs after *Zhu et al.* [2009].

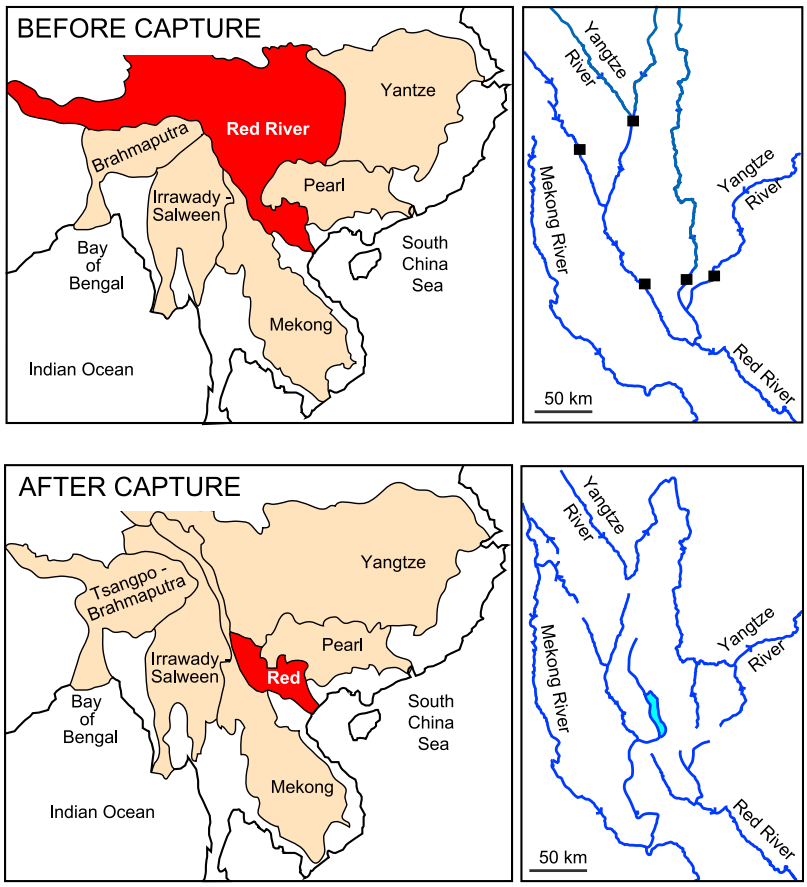

Figure 3. Cartoon after *Clark et al.* [2004] (modified by permission of American Geophysical Union) to show proposed changes to regional drainage associated with river capture and reversal connected to surface uplift of eastern Tibet. Effect of this process was to progressively shrink the drainage area leading to a catchment similar to that of the modern Red River.

migration in sedimentation seen in the Song Hong–Yinggehai Basin appears consistent with the Red River as the primary source of sediment, however, in the Pliocene there is clear evidence for erosion of Hainan Island recorded by Pliocene foresets that mostly prograde W to NW and SW away from Hainan Island [*van Hoang et al.*, 2010].

3. Approach and Methods

[9] Low temperature chronometry data are ideal for quantifying long-term (10^6–10^8 yr) depths of erosion to compare source region erosion with basin deposition volumes. Published apatite fission track (AFT) data sets exist for northern Vietnam [*Maluski et al.*, 2001; *Viola and Anczkiewicz*, 2008], central Vietnam [*Carter et al.*, 2001] and the adjacent South China margin [*X. Li et al.*, 2005; *Yan et al.*, 2009] but little is known about the exhumation history of Hainan Island hence to plug this gap samples were collected for AFT and apatite U-Th-He chronometry. The outcrop geology shows the western half of Hainan Island, closest to the Song Hong–Yinggehai Basin and the Qiongdongnan Basin further south, has experienced most erosion with exposure of bedrock that range from Palaeozoic basement to Cenozoic sedimentary rock sequences, although most outcrop comprises Triassic and Jurassic granitoids. The northern and eastern parts of the island are covered by Late Cenozoic volcanic rocks hence erosion in this area has since been low. A NE-SW oriented sample transect from the coast to the centrally located Wuzhishan Mountain (marked A-B in Figure 4) thus captures regional trends in exhumation relevant to sediment delivery to the marine basins located to the west and south of the island.

[10] U-Pb dating of detrital zircon from marine core samples were also used to directly constrain basin sediment provenance. Sampled wells, were

Table 1. Comparison of Depths of Regional Erosion for Drainage Areas Similar in Scale to the Present-Day Red River With Paleodepths of Erosion Based on Thermal History Models of Apatite Fission Track and U-Th-He Data[a]

Song Hong–Yinggehai Basin, Stratum Age (Ma)	Total Sediment Rock Volume in Basin[b] (km^3)	Total Eroded Rock Volume (km^3) Corrected for Chemical Weathering	Depth of Erosion Restricted to Paleodrainage Comparable to the Modern Red River (143,000 km^2)	Maximum Depth of Erosion Indicated by Cooling Histories of Bedrock AFT Data: Vietnam (143,000 km^2 (Equivalent to Corrected Rock Volume))	Maximum Depth of Erosion Indicated by Cooling Histories of Bedrock AFT Data: Hainan (33,920 km^2 (Equivalent to Corrected Rock Volume))
0.0–2.0	32,000	41,920			
2.0–5.5	71,000	93,010			
5.5–10.5	40,000	52,400			
10.5–15.5	64,000	83,840			
Subtotal (0.0–15.5 Ma)	207,000	271,170	1.9 km	1.5 ± 0.3 km (214,500)	1.5 ± 0.3 km (50,880)
15.5–21.0	39,000	51,090			
21.0–29.5	139,000	182,090			
Subtotal (15.5–29.5 Ma)	178,000	233,180	1.6 km	1.3 ± 0.3 km (185,900)	1.0 ± 0.2 km (33,920)
Total depth of erosion			3.5 km	2.8 ± 0.6 km	2.5 ± 0.5 km
Total volume	385,000	504,350		400,400 km^3	84,800 km^3

[a]*Maluski et al.*, 2001; *Viola and Anczkiewicz*, 2008; this study. Sediment volumes for the Song Hong–Yinggehai Basin are from *van Hoang et al.* [2010].

[b]To enable direct comparison with bedrock erosion volumes the basin volume data have also been adjusted for loss due to chemical weathering based on data from the Red River basin [*Moon et al.*, 2007]. Present-day Red River catchment area is 143,397 km^2.

mainly from the eastern margin of the basin, dictated by availability of cored sandstones and drilled depths. Although this spread cannot be used to image provenance changes through time for the entire basin the samples from the eastern margin of the basin can be used to validate sources from Hainan. Sample depositional ages are from *Yan et al.* [2007]. Figure 5 summarizes the detrital zircon U-Pb results and the raw data are provided in the auxiliary material.[1]

4. Results and Interpretation

4.1. Song Hong–Yinggehai Basin Provenance

[11] Detrital zircons extracted from core samples in the Song Hong–Yinggehai have depositional ages that range from the Late Oligocene to Pleistocene spanning the period that geochemical and isotopic studies show sediment sources switching from young (Phanerozoic) granite-dominated terrain to older (Proterozoic or Archean) crustal rocks [*Clift et al.*, 2006; *Yan et al.*, 2007]. The zircon U-Pb results (Figure 5) are dominated by zircons dated to between 90 and 110 Ma and 225–275 Ma. The Triassic and Cretaceous aged zircons are predominantly euhedral, which implies limited transport and local sources. None of the Mesozoic ages fit with rocks from northern-central Vietnam adjacent to the Red River Fault zone that are mainly Archean and Proterozoic in age [*Carter et al.*, 2001], and which dominate detrital zircon U-Pb data sets from the modern Red River and it tributaries [*van Hoang et al.*, 2009].

4.2. Hainan

[12] Zircon FT central ages from the Triassic and Jurassic igneous rocks fall between 101 ± 4 Ma and 108 ± 6 Ma and contrast with ages between 56 ± 3 Ma and 77 ± 3 for the Cretaceous granites (Table 2). The c. 100 Ma ZFT ages are similar to other ZFT data collected from along the South China margin [e.g., *X. Li et al.*, 2005; *Yan et al.*, 2009] and the emerging picture is that of a major regional cooling and inversion event which affected the entire South China margin in the Lower Cretaceous. Apatite FT central ages range from 49 ± 4 to 23 ± 2 Ma with mean track length values between 12.02 μm and 14.68 μm. Apatite He ages show a similar range of ages (Table 3) from 43 ± 2 Ma to 17 ± 1 Ma. To understand the significance of these ages in terms of sample cooling histories (where cooling is the result of erosion driven exhumation) the FT and U-Th-He data were jointly modeled.

[1]Auxiliary materials are available in the HTML. doi:10.1029/2011GC003533.

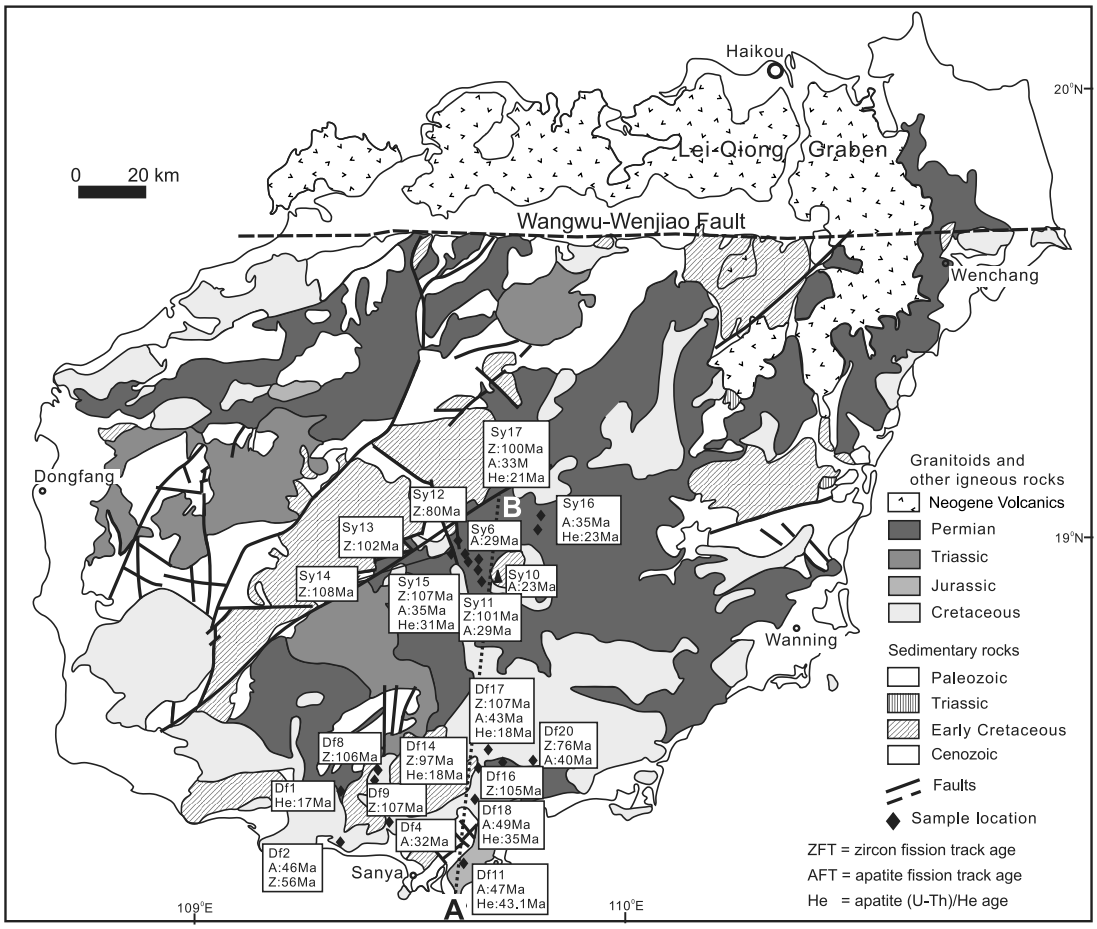

Figure 4. Geological map of Hainan showing sample locations and their fission track and U-Th-He ages.

[13] Thermal history modeling often ignores the fact that there is no unique solution to any given set of data and therefore it is preferable to adopt a modeling approach that allows for nonuniqueness to be expressed (unlike forward models where the solution is directed), and avoids adding over-complexity to the solutions (thermal history). To meet this requirement the thermal history modeling used a Bayesian, or probabilistic approach based on inversion using transdimensional Markov chain Monte Carlo (MCMC). The number of time temperature points, or the complexity of the thermal history solutions are inferred from the data rather than being specified in advance [*Gallagher et al.*, 2005, 2009; *Sambridge et al.*, 2006]. As a more general introduction to MCMC modeling the Bayesian approach allows for three different types of thermal history model which are compared to identify common features. The Maximum Likelihood Model is the best data fitting model, although this model tends to produce over complexity with features that are not justified from the data. The Maximum Posterior Model has a posterior probability that is proportional to the likelihood multiplied by the prior. For models of constant dimension (i.e., time-temperature points) and for uniform prior distributions the maximum likelihood and posterior models will be the same. The Expected Model is the preferred model which in Bayesian formulations is effectively the mean model, using all the samples from the posterior distribution. In terms of complexity this model will generally lie between the maximum likelihood model (more complex) and the maximum posterior model (less complex).

[14] Figure 6 provides a summary of the modeled thermal histories representative of the data set and sampled locations across Hainan together with uncertainties. A key advantage of using the Bayesian approach is that the expected model provides a statistical basis for calculating the uncertainty as

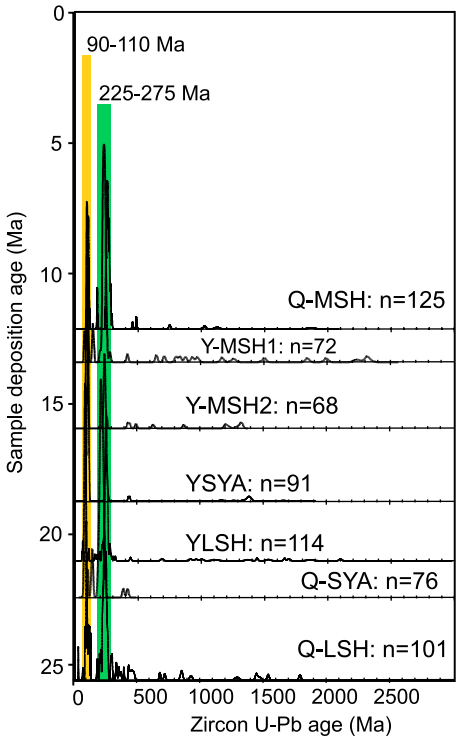

Figure 5. Probability plots of the detrital zircon data from the Song Hong–Yinggehai Basin.

credible intervals (the Bayesian equivalent of confidence intervals). These intervals represent a 95% probability range so that 2.5% of the parameter values lie below and above the limits defined by the range. A more complete thermal history that takes into account earlier events not seen by the AFT data is shown in Figure 7. This includes a Cretaceous cooling event recorded by the ZFT data that involved exhumation to surface (recorded by patches of Cretaceous sedimentary cover on some of the sampled granites) after which reburial reset the AFT system. The AFT data record cooling from this more recent reburial event. All samples exhibit a similar form of cooling history although the timing of onset of cooling is not obvious from the AFT thermal history models other than it must coincide with, or predate the oldest preserved tracks (c. 60 Ma), and postdate granite exhumation in the Lower Cretaceous (i.e., after 90 Ma) recorded by the zircon FT data. Final stage cooling rate is steady and uninterrupted apart from sample DF4 which has a hint of a small acceleration in cooling rate from circa 10–15 Ma. We converted the amounts of Cenozoic cooling recorded by the modeled data (including published data for Vietnam) for the time intervals between 0 and 15 Ma and 15–30 Ma into depths of erosion based on geothermal gradients for relatively unthinned South China crust of 35 ± 5°C/km [*Yuan et al.*, 2009]. Uncertainties for our erosion estimates take into account ±5°C for both the geothermal gradient and the thermal history cooling paths.

5. Discussion

[15] The Oligocene and Miocene core samples taken from boreholes drilled along the eastern margin of the Song Hong–Yinggehai Basin are dominated by Mesozoic aged zircons. Many have U-Pb ages between 90 and 110 Ma and Hainan Island is an obvious source given the sample locations (Figure 2) and the geology of Hainan which includes Cretaceous granitoids and volcanic rocks with similar ages to the dated detrital zircons [*S. Li et al.*, 2005; *Li et al.*, 2006; *Xie et al.*, 2005]. Most noteworthy are the kilometer thick volcanic sequences found within faulted basins in the southeast of the island (Liuluocun, Tangtadaling and Lingkecun Formations) [*Cai and Fu*, 1997] which contain zircons with U-Pb ages between 98 and 123 Ma, including a thick unit at 107 Ma [*Cai and Fu*, 1997]. Sources from the South China margin are considered unlikely given that most exposed granitoid rocks have older ages [*Li and Li*, 2007]. In addition the sediment routing would have needed to bypass the Beibu Basin (Figure 3).

[16] The detrital U-Pb data show Hainan Island was an important local source of sediment throughout the Oligocene and Miocene but this erosion would not have been distributed equally across the island due to Cenozoic volcanism and the influence of the Hainan plume [*Lei et al.*, 2009]. There were two main episodes of volcanism: In the Pliocene associated with quartz and olivine tholeiites and in the Quaternary with eruption of alkali olivine basalts and olivine tholeiites [*Ho et al.*, 2000]. Location of the volcanism appears to be influenced by the major faults which are broadly, E-W and NW-SE oriented. The E-W oriented faults (Wangwu-Wenjiao, Jianfeng-Diaoluo and Jiusuo-Lingshui faults) are significantly deeper and appear to cut through the Moho [*Lei et al.*, 2009]. The Wangwu-Wenjiao fault (Figure 4) is the most notable as it serves as a boundary between the volcanic areas to the northeast and the topographically higher granitic terrain in the central and southern parts of the island. North of the fault the depth to Moho is much shallower, crust is thinner (between 31 and 33 km), and heat flow higher, up to 87 mW/m^2 [*Lei et al.*, 2009]. These fundamental differences, either side of the Wangwu-Wenjiao fault, suggest a tilted plume, reinforced by a recent

Table 2. Fission Track Data From Hainan[a]

Sample/ Mineral	Lithology	Elevation (m asl)	Position		Number of Crystals	Dosimeter		Spontaneous		Induced		Central Age (Ma)	Age Dispersion		Mean Track Length (μm)	S.D. (μm)	Number of Tracks
			Latitude (N)	Longitude (E)		ρ_d	N_d	ρ_s	N_s	ρ_i	Ni	$\pm1\sigma$	RE%	$P\chi^2$			
SY6-Ap	Granite	481	18 53′13	109°36′05	21	1.122	7774	0.3649	357	2.372	2303	28.7 ± 1.7	0.1	90.2	13.33 ± 0.21	1.54	54
SY10-Ap	Granodiorite	632	18°54′17	109°39′07	14	1.122	7774	0.3054	307	2.497	2523	22.9 ± 1.7	14.5	14.2	13.65 ± 0.23	1.55	44
SY11-Ap	Granite	614	18°52′36	109°38′31	14	1.122	7774	0.2937	354	2.335	2822	23.2 ± 1.7	15.8	8.1	No lengths		
SY11-Zr					19	0.515	3261	17.60	4176	5.417	1250	100.9 ± 4.1	6.9	21.8			
SY12-Zr	Granodiorite	239	18°55′54	109°27′15	11	0.5133	3261	16.92	3039	6.582	1123	79.8 ± 3.9	8.3	12.4			
SY13-Zr	Diorite	203	18°55′36	109°28′30	20	0.5123	3261	15.55	3118	4.649	918	102.3 ± 4.3	0.3	83.1			
SY14-Zr	Diorite	431	18°52′29	109°30′39	20	0.5105	3261	10.65	2162	3.001	616	107 ± 5.5	5.2	31.2			
SY15-Ap	Diorite	329	18°53′44	109°30′41	21	1.122	7774	0.596	769	3.286	4200	34.6 ± 1.5	0.0	76.2	12.80 ± 0.16	1.13	50
SY15-Zr					20	0.5069	3261	16.59	3835	4.666	1070	107.4 ± 4.4	1.8	39.7			
SY16-Ap	Granodiorite	240	19°03′39	109°50′18	20	1.122	7774	0.8542	801	4.54	4202	35.2 ± 1.6	6.6	24.1	13.02 ± 0.23	1.51	45
SY17-Ap	Granodiorite	250	19°02′30	109°48′08	19	1.122	7774	0.3093	320	1.79	1842	32.7 ± 2.0	1.5	66.2	14.68 ± 0.33	1.35	17
SY17-Zr					21	0.5051	3261	9.04	2084	2.743	598	100.4 ± 5.1	0.1	80.5			
DF2-Ap	Granite	164	18°14′38	109°18′31	18	1.113	3426	0.497	173	1.193	708	45.5 ± 3.9	0.0	98.8	12.68 ± 0.23	1.24	30
DF2-Zr					20	0.5544	3842	19.52	3821	11.15	2210	56.2 ± 3.2	20.0	0.0			
DF4-Ap	Granodiorite	150	18°14′47	109°18′52	22	1.351	3746	0.5806	303	3.991	2122	32.3 ± 2.1	0.8	83.4	12.29 ± 0.15	1.50	101
DF8-Zr	Granite	235			26	0.5544	3842	21.53	5413	6.690	1663	106.6 ± 4.4	8.0	26.7			
DF9-Zr	Granite	279			14	0.5544	3842	15.29	1939	1.529	589	107.5 ± 5.8	7.6	21.62			
DF11-Ap	Granite	93	18°08′10	109°28′32	21	1.351	3746	0.167	64	0.808	309	46.8 ± 6.5	0.0	100	12.32 ± 0.39	2.35	35
DF14-Zr	Granite	335			12	0.5544	3842	25.16	2660	8.07	892	97.6 ± 4.1	0.0	97.27			
DF16-Zr	Granite	321			18	0.5544	3842	19.72	3587	6.102	1110	105.7 ± 4.1	2.6	60.6			
DF17-Ap	Granite	364	18°21′47	109°38′52	20	1.351	3746	0.457	292	2.365	1510	43.7 ± 2.9	0.2	75.11	12.52 ± 0.15	1.36	87
DF17-Zr					22	0.5544	3842	14.04	3080	4.600	1009	102.1 ± 4.3	0.0	98.22			
DF18-Ap	Granite	345	18°14′39	109°40′40	17	1.351	3746	0.3675	190	1.744	879	48.9 ± 4.0	0.2	84.43	12.65 ± 0.14	1.36	90
DF20-Ap	Granite	320	18°21′45	109°43′38	21	1.113	3426	0.486	193	2.233	901	39.9 ± 3.2	0.0	98.15	12.02 ± 0.18	1.13	40
DF20-Zr					15	0.5544	3842	18.81	2577	8.027	1101	76.6 ± 3.1	0.0	81.05			

[a]Spontaneous tracks in apatite were revealed using 5N HNO_3 at 20°C for 20 s and for zircon a eutectic of potassium hydroxide and sodium hydroxide at 225°C. Etched grain mounts were packed with mica external detectors and corning glass dosimeters (CN5 and CN2) and irradiated in the FRM 11 thermal neutron facility at the University of Munich, Germany. Ages were determined using the zeta calibration method and IUGS recommended age standards [*Hurford*, 1990]. Track densities are ($\times10^6$ tr cm^{-2}); m asl indicates meters above sea level.

Table 3. Apatite (U-Th)/He Data From Hainan[a]

Sample	Aliquot	n	He nmol/g	U (ppm)	Th (ppm)	F_T	Raw Age (Ma)	He Age (Ma)	Error Abs	S. D.	AFT Age (Ma)
SY15	A	2	0.042	1.0	1.0	0.92	31.7	34.3	2.4		
	B	2	0.109	4.9	5.2	0.91	29.8	32.8	2.3		
	C	2	0.023	1.6	2.6	0.90	24.4	27.2	1.9		
Mean			0.058	2.5	2.9	0.9	28.6	31.5	1.3	3.7	35
SY16	A	2	2.564	4.1	0.8	0.93	20.0	21.4	1.5		
	B	2	1.081	1.7	0.2	0.90	22.1	24.5	1.7		
	C[b]	2	0.865	0.0	0.0	0.93	102.4	110.3	7.7		
Mean			1.822	2.9	0.5	0.9	21.0	23.0	1.1	2.2	35
SY17	A	2	2.633	2.4	6.8	0.88	15.4	17.6	1.2		
	B	2	1.568	2.4	6.6	0.89	19.7	22.1	1.5		
	C	2	3.937	2.9	8.1	0.87	19.6	22.4	1.6		
Mean			2.713	2.6	7.2	0.9	18.3	20.7	0.8	2.7	33
DF1	A	3	0.007	1.6	5.7	0.84	13.0	15.5	1.1		
	B	2	0.012	0.4	1.5	0.91	19.3	21.2	1.5		
	C	3	0.013	1.3	4.3	0.88	13.4	15.2	1.1		
Mean			0.011	1.1	3.8	0.9	15.2	17.3	0.7	3.4	No FT age
DF11	A	3	1.543	0.9	3.4	0.78	35.8	46.0	3.2		
	B	3	1.131	0.5	2.4	0.83	33.6	40.3	2.8		
	C[b]	3	0.892	1.1	4.9	0.79	81.7	103.5	7.2		
Mean			1.337	0.7	2.9	0.8	34.7	43.1	2.1	4.0	47
DF17	A	3	1.242	3.5	12.4	0.83	16.3	19.6	1.4		
	B	3	0.998	5.9	19.3	0.84	15.6	18.6	1.3		
	C	2	2.714	4.2	14.0	0.83	12.4	14.9	1.0		
Mean			1.652	4.5	15.2	0.8	14.8	17.7	0.7	2.5	44
DF18	A	3	0.499	2.5	2.1	0.82	31.1	37.9	2.7		
	B	2	1.540	5.1	3.5	0.81	22.8	28.0	2.0		
	C	3	3.786	2.8	3.4	0.81	31.2	38.5	2.7		
Mean			1.942	3.5	3.0	0.8	28.4	34.8	1.4	5.9	49

[a]Outgassing used an induction furnace at 950°C for 15 min. The ^{4}He was measured relative to ^{3}He spike on a Pfeiffer Prisma 200 quadrupole mass spectrometer and U-Th concentrations using an Agilent 7500a quadrupole mass spectrometer. Total uncertainty on sample age is based on reproducability of Durango apatite (6.7%) combined with the U-Th and He analytical uncertainties. The standard deviation of the age replicates is used as the error when it is higher than the analytical uncertainty.
[b]Inclusion.

high-resolution tomographic model of the upper mantle that showed a low-velocity anomaly tilted to the southeast [*Lei et al.*, 2009].

[17] A tilted plume and the strong fault control explain why there is a disconnect between topography and exhumation history across Hainan Island, and why the thermochronometry data show no evidence of heating associated with the volcanism. Under normal conditions thermochronometry data would be expected to record accelerated cooling due to exhumation associated with plume uplift but the cooling recorded by AFT and AHe data in this study significantly predates the volcanism. Nevertheless, there is some independent evidence that erosion rates did increase from the Late Miocene. Seismic lines across the marginal areas of the Song Hong–Yinggehai Basin show progradational slope clinoforms coming from Hainan, as early as the Late Miocene [*Chen et al.*, 1993] and into the Pliocene [*van Hoang et al.*, 2010]. The thermochronometers are not sensitive to this increase in erosion because the magnitude of exhumation has, so far, been too small to bring rock from the AFT and U-Th-He total reset zones to the surface.

[18] Sediment isopach maps (Figure 8) constructed for the Yinggehai Basin [*Gong et al.*, 1997, 2004] show Hainan was clearly an important source of sediment and the overall contribution to basin sedimentation can be gauged from the thermochronometry results which allow for a maximum 2.5 km depth of denudation since ~30 Ma. If this depth of erosion took place across the whole island (33,920 km^2) 84,800, km^3 of rock would have been removed (Table 1), which represents 17% of the 504,350 km^3 rock equivalent of sediment deposited in the Song Hong–Yinggehai Basin since ~30 Ma. In reality Hainan would have supplied less than this as the erosion history for some of the samples extends beyond 30 Ma and land areas would have changed through time as would sea level. Some of the eroded rock would also have been transported to the north and deposited in the Beibu Basin, and to the south into the Qiongdongnan Basin hence

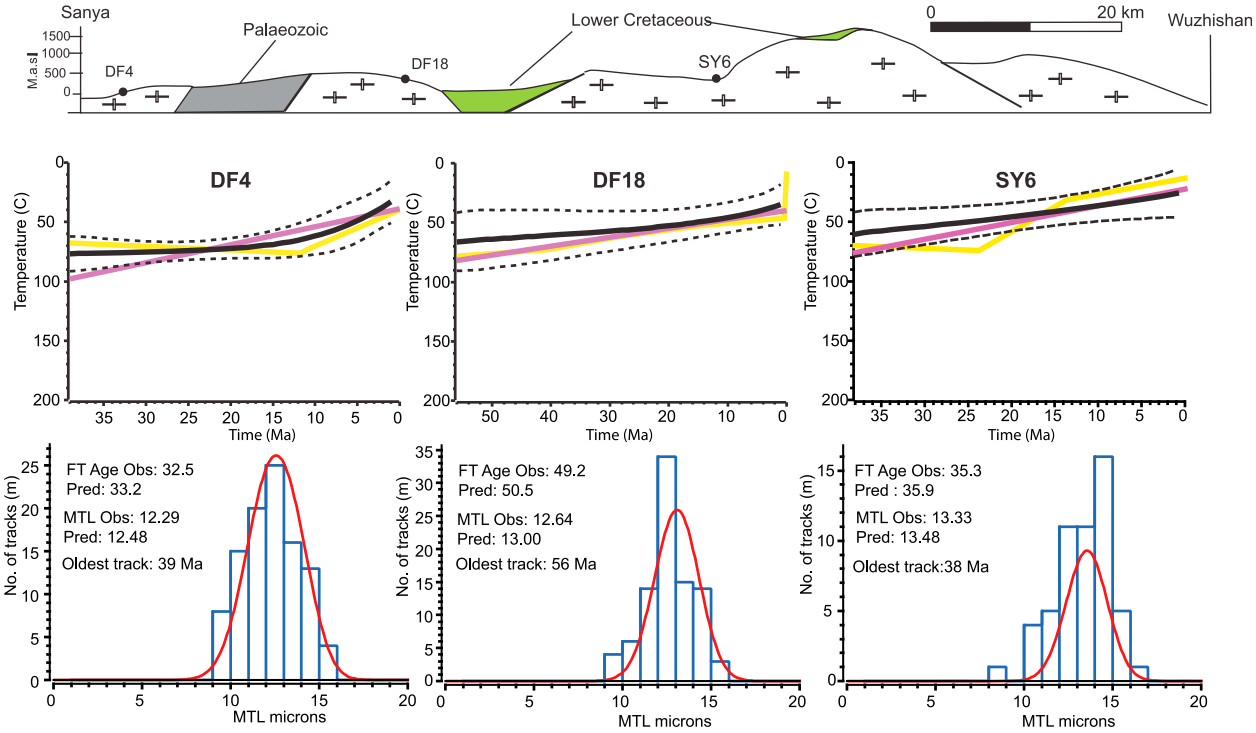

Figure 6. Representative thermal history plots for samples from Hainan produced using the procedure of *Gallagher et al.* [2005, 2009] and *Sambridge et al.* [2006].

17% is an absolute upper limit, 5–10% would seem more likely.

[19] A similar exercise can be used to assess whether the paleodrainage area was comparable to the modern Red River or if it once had a much larger catchment area that extended further north into China and east Tibet as suggested by geomorphic models [e.g., *Clark et al.*, 2004] (Figure 3). The magnitude of cooling recorded by thermal history models of published apatite fission track data collected from bedrock across the widest parts of the modern Red River drainage in north Vietnam (Figure 9) [*Maluski et al.*, 2001], and similarity of AFT ages for unmodeled data [*Viola and Anczkiewicz*, 2008], were used to define an average depth of denudation across the region since 30 Ma of 2.8 ± 0.6 km (Table 1). This depth of erosion, if confined to a drainage area similar to that of the modern Red River, would account for 80% of the sediment deposited in the Song Hong–Yinggehai Basin (Table 1).

[20] The missing 20% of sediment volume can be explained by inputs from Hainan (5–17% of the basin fill), as well as the eastern margins of Vietnam. Modern sediment flux from the Vietnamese margin outside the area of the Red River catchment includes the Da, Ma, Chu and smaller rivers. Seismic surveys show such inputs clearly existed in the past (Figure 8), for example the large clinoforms that prograde eastward away from the coast of Indochina during the Miocene [*van Hoang et al.*, 2010; *Yao et al.*, 2008]. In the northwestern part of the Song Hong–Yinggehai Basin there is a clear axial trend to basin deposition consistent with the bulk of sediment coming from the Red River region, i.e., northern Vietnam (Figures 8a and 8b). However, further south in the basin there is clear

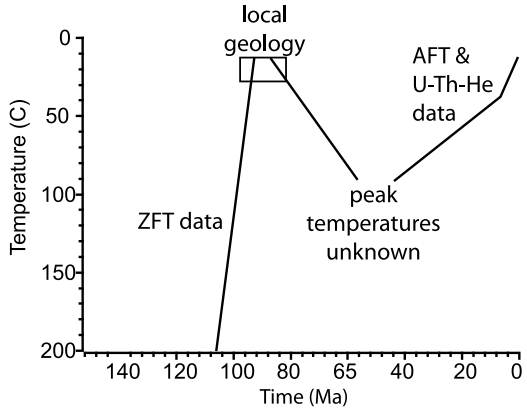

Figure 7. Summary of Hainan burial and exhumation history since the Cretaceous from ZFT, AFT, U-Th-He thermal history modeling, and outcrop geology.

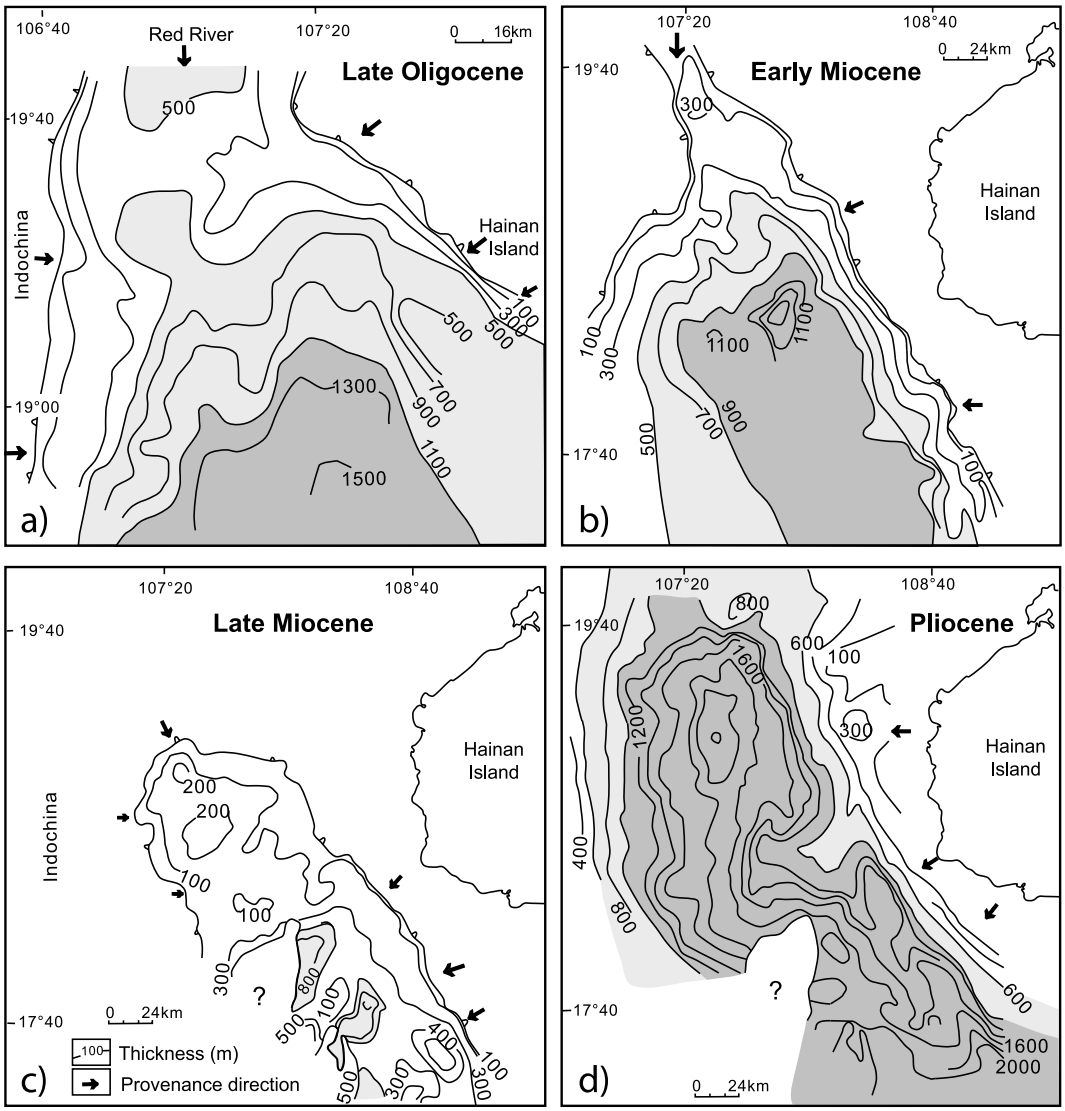

Figure 8. Sediment isopach maps for the Yinggehai Basin [*Gong and Li*, 1997, 2004] showing basin depocenter trends and the main source inputs for (a) upper Oligocene, (b) lower Miocene, (c) upper Miocene, and (d) Pliocene. Contour thicknesses are given in meters.

evidence for other sources of sediment based on contrasting sets of downlapping structures, one of which is observed trending from west to east consistent with sources from onshore eastern Vietnam, the other set in the opposite direction from Hainan to the northeast [*Xie et al.*, 2008] (Figure 8c). Unfortunately, lack of thermochronometric data from onshore eastern Vietnam means that the scale of this contribution is currently unknown. Nevertheless, it is hard to see how, based on the evidence discussed above, that the paleodrainage of the Red River could have been much larger, if at all, than the modern catchment.

[21] Given that the Song Hong–Yinggehai Basin paleodrainage would have been broadly similar in area to the current Red River catchment the sediment volumes can be converted to average long-term rates of erosion based on a catchment of similar size. This was done for the two key periods: (1) 30–15 Ma covering dextral motion on the Red River fault zone and opening of the South China Sea and (2) postrift from 15 Ma to present during which shifts in monsoon climate are widely believed to have taken place [*Wan et al.*, 2007; *Wei et al.*, 2006]. Results show total mass accumulation in the basin between 15 and 30 Ma was equivalent to 1.6 km of denudation across the source areas which compares with an average 1.3 ± 0.3 km depth of erosion calculated from the bedrock fission track data (Table 1). These two values equate to similar

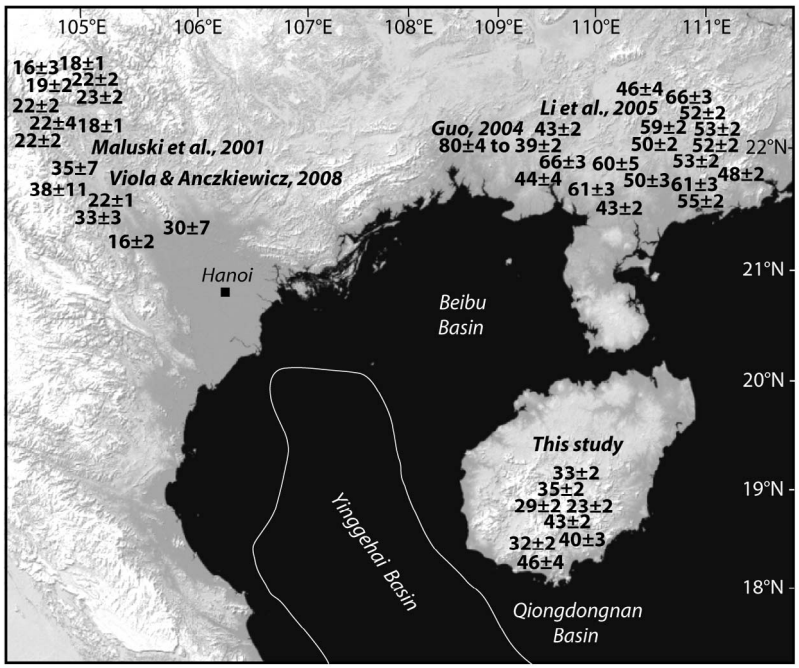

Figure 9. Summary map of published apatite fission track ages [*Guo*, 2004; *X. Li et al.*, 2005; *Maluski et al.*, 2001; *Viola and Anczkiewicz*, 2008] and the new results from Hainan.

long-term erosion rates of 107 ± 21 m/Myr and 87 ± 17 m/Myr, respectively. The scale of cooling recorded by thermochronometry models for north Vietnam since 15 Ma allow for a further 1.5 ± 0.3 km of denudation at rates of erosion of 100 ± 20 m/Myr. The sediment volume deposited in the Song Hong–Yinggehai Basin over the same time interval was equivalent to 1.9 km of denudation at an erosion rate of 127 ± 25 m/Myr, again the two values are comparable taking into account the uncertainties. Based on these observations the conclusion is that the background flux of sediment and onshore erosion did not change by very much over a period of 30 Myr.

[22] Sedimentation in the Song Hong–Yinggehai Basin is normally divided into synrift and postrift sequences since extensional tectonics appears to be the dominant control on basin formation however the pattern of sedimentation would seem more closely linked to activity on the Red River Fault zone. This is evident on seismic reflection lines that show a basin-wide angular unconformity which separates faulted Eocene to early Miocene synrift sequences from relatively uniform postrift strata. The angular unconformity formed between 21 and 16 Ma as fast sinistral slip of the Red River Fault ended. After 16 Ma slip reversal took place until 5.5 Ma when slip rates slowed [*Zhu et al.*, 2009]. These changes affected basin sedimentation by causing a general migration of depocenters to the southeast until fault reversal at 16 Ma halted this trend and caused depocenters to move back to the northwest until fault movement slowed down and rates of sediment supply led to overspill to the east into the Qiongdongnan basin [*Clift and Sun*, 2006; *Xie et al.*, 2008; *Zhu et al.*, 2009].

[23] During the period of sinistral slip the Song Hong–Yinggehai Basin recorded the highest sediment accumulation rates (c. 200 g cm^{-2} ka^{-1} and up to 8.5 km of sedimentation) of all the South China Sea basins [*Huang and Wang*, 2006], which implies high rates of denudation in the sources areas. Studies have tended to link this rapid erosion to increased exhumation across the onshore RRFZ spanning the Day Nui Con Voi massif in Vietnam and the southern segment of the Ailao Shan in China [*Zhu et al.*, 2009]. This is not unreasonable given that the AFT data from across the RRFZ [*Maluski et al.*, 2001] record two phases of cooling during the Cenozoic that correlate with fault activity. An early phase of exhumation during the Oligocene is associated with emplacement of the Phan Si Pang granite followed by a later acceleration of exhumation, dated to between 25 and 21 Ma, confined to the Day Nui Con Voi shear zone. Both pulses of cooling correspond to changes in slip rate along the main fault which *Harrison et al.* [1996] noted also coincides with a transtensional phase

and which later studies showed had a regional NE-SW oriented extension component [*Viola and Anczkiewicz*, 2008].

[24] Changes in Song Hong–Yinggehai Basin sediment flux since 16–15 Ma have also been major points of discussion in previous studies, especially the apparent increase in sediment accumulation rates that took place between 15.5 and 10 Ma when a shift in monsoon intensity is thought to have occurred [*Clift and Sun*, 2006; *van Hoang et al.*, 2010]. However, the long-term erosion rates calculated by this study reveal no major changes before or after 15 Ma and this suggests that monsoon forcing of erosion rates was not significant and that short-term shifts in sediment flux likely have other more local causes. Reorganizations in the paleodrainage system are ruled out due to the mass balance between the onshore denudation records and basin sediment volumes. Sea level forcing may have had an influence as there were small-scale (<20 m) shifts in sea level between 15 and 10 Ma, but depocenter adjustments related to changes in motion along the offshore part of the Red River Fault zone were likely more important.

6. Conclusions

[25] Previous studies of sediment mass accumulation in the Song Hong–Yinggehai Basin have drawn attention to short-lived (few Myr) fluctuations in sediment flux, mostly in the middle Miocene, and have suggested that these changes might be related to monsoon intensity forcing the erosion. The large volume of sediment has also been considered to be the product of a much larger paleo Red River that once connected drainage of the eastern margins of the Tibetan plateau to the South China Sea. To test these interpretations we compared basin mass accumulation with erosion histories of source regions across northern Vietnam and Hainan Island. We found that depths of erosion since 30 Ma in northern Vietnam, averaged over an area similar to that of the modern Red River catchment, can account for 80% of the sediment deposited in the Song Hong–Yinggehai Basin. The residual 20% can be explained by contributions from Hainan Island and the eastern margin of Vietnam. Thus, if a significantly expanded paleodrainage ever existed, it must have predated the Oligocene. We also found similar average depths of erosion (1.6 km and 1.3 km) across the modern Red River drainage area before rifting and active sinistral motion on the Red River fault zone (30–15.5 Ma) and after (15.5 Ma to present). This finding suggests that any short-lived shifts in monsoon intensity or tectonics had no lasting impact on background long-term erosion rates.

Acknowledgments

[26] This work was financially cosupported by the National Natural Science Foundation of China (Grant 40972130), Major State Basic Research Program of the People's Republic of China (2009CB219401), and NSFC-UK Royal Society Joint Project award (40811130248). This is contribution (GIGRC-10-01) IS-1338 from GIGCAS.

References

Cai, D. G., and G. X. Fu (1997), Classification and correlation of Tong'anling Niulaling volcanic strata in southern Hainan, *Geol. Bull. China*, *16*, 348–358.

Carter, A., D. Roques, P. Kinny, and C. S. Bristow (2001), Understanding Mesozoic accretion in Southeast Asia: Significance of Triassic thermotectonism in Vietnam, *Geology*, *29*, 211–214, doi:10.1130/0091-7613(2001)029<0211:UMAISA>2.0.CO;2.

Chen, P. H., Z. Y. Chen, and Q. M. Zhang (1993), Sequence stratigraphy and continental margin development of the northwestern Shelf of the South China Sea, *Am. Assoc. Pet. Geol. Bull.*, *77*, 842–862.

Clark, M. K., L. M. Schoenbohm, L. H. Royden, K. X. Whipple, B. C. Burchfiel, X. Zhang, W. Tang, E. Wang, and L. Chen (2004), Surface uplift, tectonics, and erosion of eastern Tibet from large-scale drainage patterns, *Tectonics*, *23*, TC1006, doi:10.1029/2002TC001402.

Clift, P. D. (2006), Controls on the erosion of Cenozoic Asia and the flux of clastic sediment to the ocean, *Earth Planet. Sci. Lett.*, *241*, 571–580, doi:10.1016/j.epsl.2005.11.028.

Clift, P. D., and Z. Sun (2006), The sedimentary and tectonic evolution of the Yinggehai–Song Hong basin and the southern Hainan margin, South China Sea: Implications for Tibetan uplift and monsoon intensification, *J. Geophys. Res.*, *111*, B06405, doi:10.1029/2005JB004048.

Clift, P. D., J. Blusztajn, and A. D. Nguyen (2006), Large-scale drainage capture and surface uplift in eastern Tibet–SW China before 24 Ma inferred from sediments of the Hanoi Basin, Vietnam, *Geophys. Res. Lett.*, *33*, L19403, doi:10.1029/2006GL027772.

Clift, P. D., V. L. Hoang, R. Hinton, R. Ellam, R. Hannigan, M. T. Tan, and D. A. Nguyen (2008a), Evolving east Asian river systems reconstructed by trace element and Pb and Nd isotope variations in modern and ancient Red River–Song Hong sediments, *Geochem. Geophys. Geosyst.*, *9*, Q04039, doi:10.1029/2007GC001867.

Clift, P., G. H. Lee, N. Anh Duc, U. Barckhausen, H. Van Long, and S. Zhen (2008b), Seismic reflection evidence for a Dangerous Grounds miniplate: No extrusion origin for the South China Sea, *Tectonics*, *27*, TC3008, doi:10.1029/2007TC002216.

Gallagher, K., J. Stephenson, R. Brown, C. Holmes, and P. Fitzgerald (2005), Low temperature thermochronology and modeling strategies for multiple samples 1: Vertical profiles, *Earth Planet. Sci. Lett.*, *237*, 193–208, doi:10.1016/j.epsl.2005.06.025.

Gallagher, K., K. Charvin, S. Nielsen, M. Sambridge, and J. Stephenson (2009), Markov chain Monte Carlo (MCMC) sampling methods to determine optimal models, model resolution and model choice for Earth Science problems, *J. Mar. Pet. Geol.*, *26*, 525–535, doi:10.1016/j.marpetgeo.2009.01.003.

Gilley, L. D., T. M. Harrison, P. H. Leloup, F. J. Ryerson, O. M. Lovera, and J. H. Wang (2003), Direct dating of left lateral deformation along the Red River shear zone, China and Vietnam, *J. Geophys. Res.*, *108*(B2), 2127, doi:10.1029/2001JB001726.

Gong, Z., and S. Li (1997), *Continental Margin Basin Analysis* and Hydrocarbon *Accumulation* of the *Northern South China Sea* [in Chinese with English abstract], Science Press, Beijing, 510 pp.

Gong, Z., and S. Li (2004), *Dynamic Research of Oil and Gas Accumulation in Northern Marginal Basins of South China Sea* [in Chinese with English abstract], Science Press, Beijing, 339 pp.

Guo, T. L. (2004), Meso-Cenozoic tectono-thermal history of Shiwandashan Basin, South China, Ph.D. thesis, School of Ocean and Earth Sci., Tongji Univ., Shanghai, China.

Guo, L., Z. Zhong, and L. Wang (2001), Regional tectonic evolution around Yinggehai basin of South China Sea, *J. China Univ. Geol.*, *7*, 1–12.

Hao, F., S. T. Li, Y. C. Sun, and Q. M. Zhang (1998), Geology, compositional heterogeneities, and geochemical origin of the Yacheng gas field, Qiongdongnan basin, South China Sea, *Am. Assoc. Pet. Geol. Bull.*, *82*, 1372–1384.

Harrison, M. T., P. H. Leloup, F. J. Ryerson, P. Tapponnier, R. Lacassin, and C. Wenji (1996), Diachronous initiation of transtension along the Ailao Shan–Red River shear zone, Yunnan and Vietnam, in *The Tectonic Evolution of Asia*, edited by A. Yin and T. M. Harrison, pp. 110–137, Cambridge Univ. Press, New York.

Ho, K., J. Chen, and W. Juang (2000), Geochronology and geochemistry of late Cenozoic basalts from the Leiqiong area, southern China, *J. Asian Earth Sci.*, *18*, 307–324, doi:10.1016/S1367-9120(99)00059-0.

Huang, W., and P. Wang (2006), Sediment mass and distribution in the South China Sea since the Oligocene, *Sci. China, Ser. D, Earth Sci.*, *49*(11), 1147–1155.

Hurford, A. J. (1990), Standardization of fission track dating calibration: Recommendation by the Fission Track Working Group of the IUGS subcommission on geochronology, *Chem. Geol.*, *80*, 177–178.

Lei, J., D. Zhao, B. Steinberger, B. Wu, F. Shen, and Z. Li (2009), New seismic constraints on the upper mantle structure of the Hainan plume, *Phys. Earth Planet. Inter.*, *173*, 33–50, doi:10.1016/j.pepi.2008.10.013.

Leloup, P. H., R. Lacassin, P. Tapponnier, U. Schärer, Z. Dalai, L. Xiaohan, Z. Liangshang, J. Shaocheng, and P. T. Trinh (1995), The Ailao Shan-Red River shear zone (Yunnan, China), Tertiary transform boundary of Indochina, *Tectonophysics*, *251*, 3–84, doi:10.1016/0040-1951(95)00070-4.

Leloup, P. H., N. Arnaud, R. Lacassin, J. R. Kienast, T. M. Harrison, T. P. Trong, A. Replumaz, and P. Tapponnier (2001), New constraints on the structure, thermochronology, and timing of the Ailao Shan-Red River shear zone, SE Asia, *J. Geophys. Res.*, *106*, 6683–6732, doi:10.1029/2000JB900322.

Li, S., Y. Yun, Y. Fan, and J. B. Zhou (2005), Zircon U-Pb age and its geological significance for Qiongzhong pluton in Qiongzhong area, Hainan Island [in Chinese with English abstract], *Geotectonica Metallogenia*, *29*(2), 227–233.

Li, X. H., G. J. Wei, L. Shao, Y. Liu, X. R. Liang, Z. M. Jian, M. Sun, and P. X. Wang (2003), Geochemical and Nd isotopic variations in sediments of the South China Sea: a response to Cenozoic tectonism in SE Asia, *Earth Planet. Sci. Lett.*, *211*, 207–220.

Li, X., Y. Wang, K. Tan, and T. Peng (2005), Meso-Cenozoic uplifting and exhumation on Yunkaidashan: Evidence from fission track thermochronology, *Chin. Sci. Bull.*, *50*(9), 903–909, doi:10.1360/04wd0040.

Li, X.-H., Z.-X. Li, W.-X. Li, and Y. Wang (2006), Initiation of the Indosinian Orogeny in South China: Evidence for a Permian magmatic arc in the Hainan Island, *J. Geol.*, *114*(3), 341–353, doi:10.1086/501222.

Li, Z.-X., and X.-H. Li (2007), Formation of the 1300-km-wide intracontinental orogen and postorogenic magmatic province in Mesozoic South China: A flat-slab subduction model, *Geology*, *35*, 179–182, doi:10.1130/G23193A.1.

Maluski, H., C. Lepvrier, L. Jolivet, A. Carter, D. Roques, O. Beyssac, T. T. Tang, N. D. Thang, and D. Avigad (2001), Ar-Ar and fission-track ages in the Song Chay massif: Early Triassic and Cenozoic tectonics in northern Vietnam, *J. Asian Earth Sci.*, *19*, 233–248, doi:10.1016/S1367-9120(00)00038-9.

Molnar, P., and P. Tapponnier (1975), Cenozoic tectonics of Asia: Effects of a continental collision, *Science*, *189*(4201), 419–426.

Moon, S., Y. Huh, J. Qin, and N. V. Pho (2007), Chemical weathering in the Hong (Red) River basin: Rates of silicate weathering and their controlling factors, *Geochim. Cosmochim. Acta*, *71*, 1411–1430, doi:10.1016/j.gca.2006.12.004.

Morley, C. K. (2002), A tectonic model for the Tertiary evolution of strike-slip faults and rift basins in SE Asia, *Tectonophysics*, *347*, 189–215, doi:10.1016/S0040-1951(02)00061-6.

Replumaz, A., and P. Tapponnier (2003), Reconstruction of the deformed collision zone between India and Asia by backward motion of lithospheric blocks, *J. Geophys. Res.* *108*(B6), 2285, doi:10.1029/2001JB000661.

Richardson, N. J., A. L. Densmore, D. Seward, M. Wipf, and Y. Li (2010), Did incision of the Three Gorges begin in the Eocene?, *Geology*, *38*(6), 551–554, doi:10.1130/G30527.1.

Sambridge, M., K. Gallagher, A. Jackson, and P. Rickwood (2006), Trans-dimensional inverse problems, model comparison and the evidence, *Geophys. J. Int.*, *167*, 528–542, doi:10.1111/j.1365-246X.2006.03155.x.

Searle, M. P. (2006), Role of the Red River shear zone, Yunnan and Vietnam, in the continental extrusion of SE Asia, *J. Geol. Soc.*, *163*, 1025–1036, doi:10.1144/0016-76492005-144.

Searle, M. P., M.-W. Yeh, T.-H. Lin, and S.-L. Chung (2010), Structural constraints on the timing of left-lateral shear along the Red River shear zone in the Ailao Shan and Diancang Shan Ranges, Yunnan, SW China, *Geosphere*, *6*, 316–338, doi:10.1130/GES00580.1.

Sun, Z., D. Zhou, Z. Zhong, Z. Zeng, and S. Wu (2003), Experimental evidence for the dynamics of the formation of the Yinggehai Basin, NW South China Sea, *Tectonophysics*, *372*, 41–58, doi:10.1016/S0040-1951(03)00230-0.

Sun, Z., Z. Zhong, D. Zhou, and Z. Zeng (2004), Continent-ocean interactions along the Red River fault zone, South China Sea, in *Continent-Ocean Interactions Within East Asian Marginal Seas*, *Geophys. Monogr. Ser.*, vol. 149, edited by P. Clift et al., pp. 109–120, AGU, Washington, D. C.

Tapponnier, P., G. Peltzer, and R. Armijo (1986), On the mechanics of the collision between India and Asia, in *Collision Tectonics*, edited by M. P. Coward and A. C. Ries, *Geol. Soc. Spec. Publ.*, *19*, 115–157.

Tapponnier, P., R. Lacassin, P. H. Leloup, U. Schärer, Z. Dalai, W. Haiwei, L. Xiaohan, J. Shaocheng, Z. Lianshang, and Z. Jiayou (1990), The Ailao Shan/Red River metamorphic belt: Tertiary left-lateral shear between Indochina and South China, *Nature*, *343*, 431–437, doi:10.1038/343431a0.

Tapponnier, P., Z. Xu, F. Roger, B. Meyer, N. Arnaud, G. Wittlinger, and J. Yang (2001), Oblique stepwise rise and growth of the Tibet Plateau, *Science*, *294*, 1671–1677, doi:10.1126/science.105978.

van Hoang, L., F.-Y. Wu, P. D. Clift, A. Wysocka, and A. Swierczewska (2009), Evaluating the evolution of the Red River system based on in situ U-Pb dating and Hf isotope analysis of zircons, *Geochem. Geophys. Geosyst.*, *10*, Q11008, doi:10.1029/2009GC002819.

van Hoang, L., P. D. Clift, A. M. Schwab, M. Huuse, D. A. Nguyen, and Z. Sun (2010), Large-scale erosional response of SE Asia to monsoon evolution reconstructed from sedimentary records of the Song Hong–Yinggehai and Qiongdongnan basins, South China Sea, in *Monsoon Evolution and Tectonic–Climate Linkage in Asia*, edited by P. D. Clift, R. Tada, and H. Zheng, *Geol. Soc. Spec. Publ*, *342*, 219–244.

Viola, G., and R. Anczkiewicz (2008), Exhumation history of the Red River shear zone in northern Vietnam: New insights from zircon and apatite fission-track analysis, *J. Asian Earth Sci.*, *33*, 78–90, doi:10.1016/j.jseaes.2007.08.006.

Wan, S., A. Li, P. D. Clift, and J.-B. W. Stuut (2007), Development of the East Asian Monsoon: Mineralogical and sedimentologic records in the northern South China Sea since 20 Ma, *Palaeogeogr. Palaeoclimatol. Palaeoecol.*, *254*, 561–582, doi:10.1016/j.palaeo.2007.07.009.

Wang, E., and B. C. Burchfiel (1997), Interpretation of Cenozoic tectonics in the right lateral accommodation zone between the Ailao Shan Shear zone and the Eastern Himalayan Syntaxis, *Int. Geol. Rev.*, *39*, 191–219, doi:10.1080/00206819709465267.

Wei, G., X. H. Li, Y. Liu, L. Shao, and X. Liang (2006), Geochemical record of chemical weathering and monsoon climate change since the early Miocene in the South China Sea,*Paleoceanography*, *21*, PA4214, doi:10.1029/2006PA001300.

Xie, C. F., J. C. Zhu, Z. J. Zhao, S. J. Ding, T. A. Fu, Z. H. Li, Y. M. Zhang, and D. P. Yu (2005), Zircon SHRIMP U-Pb age dating of garnet-acmite syenite: Constraints on the Hercynian-Indosinian tectonic evolution of Hainan Island, *J. China Univ. Geol.*, *11*(1), 47–57.

Xie, X., S. Li, W. Dong, and Z. Hu (2001), Evidence for episodic expulsion of hot fluids along faults near diapiric structure of the Yinggehai basin, South China, *Mar. Pet. Geol.*, *18*, 715–728, doi:10.1016/S0264-8172(01)00024-1.

Xie, X., R. D. Muller, J. Ren, T. Jiang, and C. Zhang (2008), Stratigraphic architecture and evolution of the continental slope system in offshore Hainan, northern South China Sea, *Mar. Geol.*, *247*, 129–144, doi:10.1016/j.margeo.2007.08.005.

Yan, Y., B. G. Xia, A. Lin, A. Carter, X. Hu, B. Liu, X. Cui, P. Yan, and Z. Song (2007), Geochemical and Nd isotope compositions of detrital sediments on the north margin of the South China Sea: Provenance and tectonic implications, *Sedimentology*, *54*, 1–17, doi:10.1111/j.1365-3091.2006.00816.x.

Yan, Y., A. Carter, L. Ge, S. Brichau, and H. Xiaoqiong (2009), Fission-track and (U-Th)/He thermochronometry of onshore South China Sea: Implication to morphotectonic evolution and sediment contribution to the northern South China Sea, *Tectonophysics*, *424*, 584–594, doi:10.1016/j.tecto.2009.04.030.

Yao, G.-S., S.-Q. Yuan, S.-U. Wu, and C. Zhong (2008), Double provenance depositional model and exploration prospect in deepwater area of Qiongdongnan Basin, *Pet. Explor. Dev.*, *35*, 685–691, doi:10.1016/S1876-3804(09)60101-4.

Yuan, Y., W. Zhu, L. Mi, G. Zhang, S. Hu, and L. He (2009), Uniform geothermal gradient and heat flow in the Qiongdongnan and Pearl River Mouth Basins of the South China Sea Marine and Petroleum, *Geology*, *26*, 1152–1162.

Zhu, M., S. Graham, and T. McHargue (2009), The Red River Fault zone in the Yinggehai Basin, South China Sea, *Tectonophysics*, *476*, 397–417, doi:10.1016/j.tecto.2009.06.015.